

Groupe d'Annecy

Laboratoire
d'Annecy-le-Vieux de
Physique des Particules

ENSLAPP

Groupe de Lyon

Ecole Normale
Supérieure de Lyon

Some aspects of thermal field theories*

P. Aurenche¹

Laboratoire de Physique Théorique ENSLAPP[†]

¹ Groupe d'Annecy: LAPP, BP 110, F-74941 Annecy-le-Vieux Cedex, France.

Abstract

Different formalisms used in the perturbative approach to Thermal Field Theory (TFT) are briefly reviewed. The rate of production of a virtual photon in a quark-gluon plasma is then discussed to illustrate some features of TFT before introducing the Hard Thermal Loop resummation which improves the behaviour of the theory in the infrared sector. Some of the successes of this approach are described before turning to the problems associated to the undamped transverse gluon oscillations and the light-cone singularities arising when on-shell and/or massless particles are involved.

hep-ph/9612432
ENSLAPP-A-624/96
November 1996

*Talk presented at the Fourth Workshop in High Energy Physics Phenomenology (WHEPP 4), Calcutta, January 1996

[†]URA 14-36 du CNRS, associée à l'Ecole Normale Supérieure de Lyon et à l'Université de Savoie.

1 Introduction

Thermal Field Theories (TFT) represent a very wide subject and only a few aspects will be touched upon in these notes. The physical systems considered will be the hot QCD (quark-gluon) plasma or the hot QED (electron-photon) plasma in equilibrium. To probe the properties of the plasma one often studies rare processes in the plasma which do not disturb the thermal equilibrium. As an illustration of such processes we shall consider the production of real or virtual (lepton pair) photons in a QCD plasma. The rate of production is proportionnal to e^2 , where e , the electric charge, is taken to be $e \ll g$, with g the strong interaction coupling which is characteristic of forces maintaining the plasma in equilibrium.

The following discussion will be based on perturbation theory and its improvements. The main problem one encounters in such an approach is that of divergences, both of the infra-red and the collinear types, related to the masslessness of quarks and gluons. First the Feynman rules at finite temperature will be introduced and several versions of them will be presented depending on the formalism used: imaginary-time formalism (ITF), real-time formalism (RTF), retarded/advanced (R/A) formalism. The production of a virtual photon in a QCD plasma will be discussed and contrasted with the case at zero temperature. The improvement of perturbation theory when soft momenta are involved is presented: this is the hard thermal loop (HTL) resummation of Braaten-Pisarski and Frenkel and Taylor and some consequences are discussed. Further problems associated to mass singularities are discussed and the need to go beyond the HTL scheme is stressed.

2 Feynman rules

Thermal field theory is the application of the technics of usual quantum field theory which describes the interactions among a few fundamental “particles”, to the study of systems characterized by a large number of particles (statistical systems) at a given temperature (thermal equilibrium is assumed) [1, 2, 3]. The thermal expectation value of an operator A is defined by:

$$\begin{aligned} \langle A \rangle_\beta &= Z^{-1} \text{Tr}(e^{-\beta H} A) \\ &= Z^{-1} \sum_m e^{-\beta E_m} \langle m | A | m \rangle \end{aligned} \quad (1)$$

where the partition function is $Z = \text{Tr}(e^{-\beta H})$, with $\beta = 1/T$ the inverse of the temperature. If one remembers the time evolution for an operator in the Heisenberg representation

$$e^{iHt'} A(t) e^{-iHt'} = A(t + t') \quad (2)$$

then one can write

$$e^{\beta H} A(t) e^{-\beta H} = A(t - i\beta) \quad (3)$$

and interpret the inverse temperature as an imaginary time. In TFT it is then natural to introduce a complex time variable, the imaginary part of which being related to the temperature.

Consider now the thermal expectation value of a bilocal operator

$$\begin{aligned}
\langle A(t)B(t') \rangle_\beta &= Z^{-1} \text{Tr} \left(e^{-\beta H} A(t)B(t') \right) \\
&= Z^{-1} \text{Tr} \left(e^{-\beta H} e^{\beta H} B(t') e^{-\beta H} A(t) \right) \\
&= \langle B(t' - i\beta)A(t) \rangle_\beta
\end{aligned} \tag{4}$$

where the property of the cyclicity of the trace has been used. This equation summarizes the important Kubo-Martin-Schwinger (KMS) condition which expresses thermal equilibrium. Projecting on complete sets of states and introducing the evolution operators, the correlation function can be written as

$$\begin{aligned}
\langle A(t)B(t') \rangle_\beta &= Z^{-1} \sum_m e^{-\beta E_m} \langle m|A(t)B(t')|m \rangle \\
&= Z^{-1} \sum_{m,n} e^{-iE_n(t-t')} e^{iE_m(t-t'+i\beta)} \langle m|A(0)|n \rangle \langle n|B(0)|m \rangle .
\end{aligned} \tag{5}$$

For this expression to be defined, the exponentials should be well behaved when $E_m \rightarrow \infty$ and this requires

$$-\beta \leq \text{Im}(t - t') \leq 0. \tag{6}$$

We turn now to a scalar field theory where $\phi(x)$ is a real field. The propagator is

$$\begin{aligned}
\langle G_c(x - x') \rangle_\beta &= \langle \theta_c(t - t') \phi(x) \phi(x') + \theta_c(t' - t) \phi(x') \phi(x) \rangle_\beta \\
&= \langle \theta_c(t - t') G^+(x - x') + \theta_c(t' - t) G^-(x - x') \rangle_\beta .
\end{aligned} \tag{7}$$

Remembering that the time variable can be complex, the time ordering operator T_c , implied by the function $\theta_c(t - t')$, generalizes on an oriented contour C in the complex time plane, the time ordering operator defined on the real axis. Then, according to eq. (6) the oriented contour has to be descending. The application of the KMS condition to the thermal propagator leads to the relations

$$G^-(t - t') = G^+(t - i\beta - t') \quad \text{and} \quad G^+(t - t') = G^-(t - t' + i\beta). \tag{8}$$

One obtains the propagator and other Green functions from the generating functional

$$Z[j] = \text{Tr} \left(e^{-\beta H} T_c \exp \left(i \int_c d^4x j(x) \hat{\phi}(x) \right) \right) \tag{9}$$

by the usual differentiation formula

$$G_c(x_1, \dots, x_n) = \frac{1}{Z[0]} \frac{\delta^n \ln(Z[j])}{i\delta j(x_1) \dots i\delta j(x_n)} \tag{10}$$

Introducing the eigenvalue of the field operator $\hat{\phi}$ at some initial time t_i

$$\hat{\phi}(x) |\phi(\vec{x}, t_i) \rangle = \phi(\vec{x}) |\phi(\vec{x}, t_i) \rangle \tag{11}$$

one has to evaluate

$$\begin{aligned} Z[j] &= \int d\phi \langle \phi, t_i | e^{-\beta H} T_c \exp \left(i \int_c d^4 x j(x) \phi(\vec{x}) \right) | \phi, t_i \rangle \\ &= \int d\phi \langle \phi, t_i - i\beta | T_c \exp \left(i \int_c d^4 x j(x) \phi(\vec{x}) \right) | \phi, t_i \rangle . \end{aligned} \quad (12)$$

Using well-known technics of splitting the time interval in small intervals one re-writes the generating functional as a functional integral

$$Z[j] = N \int [\mathcal{D}(\phi)] \exp i \int_c d^4 x (\mathcal{L}(x) + j(x)\phi(x)) \quad (13)$$

where the time contour runs from t_i to $t_i - i\beta$ and the fields are subject to the periodic boundary condition

$$\phi(t_i, \vec{x}) = \phi(t_i - i\beta, \vec{x}) \quad (14)$$

because of the same “initial” and “final” state as implied by the Trace operation. From now on, one constructs the perturbative expansion, as in the zero temperature case, by decomposing the lagrangian into its free part and its interacting part.

We concentrate now on the construction of the propagator before specifying the contour which will lead to the different formalisms mentioned in the introduction. First, introduce the Fourier transform of the functions G_c^\pm

$$D^\pm(K) = \int d^4 x e^{iKx} G_c^\pm(x). \quad (15)$$

The KMS conditions easily give the relation

$$D^-(K) = e^{\beta k_0} D^+(K) \quad (16)$$

and defining now the spectral function $\rho(K) = D^+(K) - D^-(K)$ one derives

$$\begin{aligned} D^-(K) &= \rho(K) n_B(k_0), \quad \text{with } n_B(k_0) = \frac{1}{e^{\beta k_0} - 1} \\ D^+(K) &= \rho(K) (n_B(k_0) + 1) \end{aligned} \quad (17)$$

and in the space-time representation

$$G_c(x) = \int \frac{d^4 K}{(2\pi)^4} e^{-iKx} \rho(K) (\theta_c(t) + n_B(k_0)). \quad (18)$$

To obtain the free field propagator one expands the field into the creation and annihilation operators:

$$\phi(x) = \int \frac{d^4 K}{(2\pi)^4} 2\pi \theta(k_0) \delta(K^2 - m^2) [a(K) e^{-iKx} + a^\dagger(K) e^{iKx}] \quad (19)$$

and one constructs the propagator from its definition eq. (7). Making use of the usual commutation relations, *e. g.*,

$$[a(K), a^\dagger(K')] = (2\pi)^3 2\omega_k \delta(\vec{k} - \vec{k}') \quad (20)$$

one finds the general expression

$$G_c(x-y) = \int \frac{d^4 K}{(2\pi)^3} e^{-iK(x-y)} \epsilon(k^0) \delta(K^2 - m^2) (\theta_c(x^0 - y^0) + n_B(k_0)). \quad (21)$$

One immediately obtains the spectral function of the free propagator to be

$$\rho(K) = 2\pi \epsilon(k^0) \delta(K^2 - m^2). \quad (22)$$

To proceed further with actual calculations it is necessary to choose a contour and this will lead to the different formalisms with different expressions for the Green's functions. Of course, the predictions for rates or cross sections should be independent of the choice of the contour.

2.1 The imaginary-time formalism

This is based on the simplest contour, running vertically in the time interval $[0, -i\beta]$ [1, 2, 4]. It is convenient to introduce the “imaginary” time τ , related to the “real” time by $t = -i\tau$. Using the KMS conditions one shows that the propagator is a periodic function of the energy of period $2\pi i/\beta$. The propagator is expanded as a Fourier series with the Matsubara frequencies $\omega_n = 2\pi n/\beta$ and one has

$$G(\tau, \vec{x}) = \frac{i}{\beta} \sum_{n=-\infty}^{\infty} \int \frac{d^3 k}{(2\pi)^3} e^{-i\omega_n \tau} e^{i\vec{k}\vec{x}} \Delta(i\omega_n, \vec{x}) \quad (23)$$

or equivalently

$$\Delta(i\omega_n, \vec{x}) = \int_0^\beta d\tau \int d^3 x e^{i\omega_n \tau} e^{-i\vec{k}\vec{x}} G(\tau, \vec{x}). \quad (24)$$

Using eq. (21) with $\theta_c(x^0 - y^0) = 1$ when $0 \leq \tau \leq \beta$ one finds:

(i) propagator:

$$\Delta(i\omega_n, \vec{k}) = \frac{i}{(i\omega_n)^2 - \omega_k^2} \quad \text{with} \quad \omega_k^2 = \vec{k}^2 + m^2;$$

(ii) vertex: $-ig$ as at $T = 0$;

(iii) energy-momentum conservation: $(2\pi)^4 \delta(K) \rightarrow -i\beta \delta_{n,0} (2\pi)^3 \delta(\vec{k})$;

(iv) loop integral:

$$\int \frac{d^4 K}{(2\pi)^4} \rightarrow \frac{i}{\beta} \sum_{n=-\infty}^{\infty} \int \frac{d^3 k}{(2\pi)^3} \quad .$$

When working in the ITF an analytical continuation to real external energy variables must be performed

$$i\omega_n \rightarrow k^0 \pm i\varepsilon, \quad \varepsilon \rightarrow 0_+, \quad (25)$$

corresponding to “retarded” and “advanced” energies.

2.2 The real-time formalism

The idea is to include the real axis in the oriented time contour as shown in Fig. 1 [3, 4]. The arbitrary parameter σ is such that $0 \leq \sigma \leq \beta$. It is convenient to introduce the following propagators depending of the relative position of x and y (see Fig. 1 for the label of the various pieces of the contour):

- (i) if x, y on C_1 $G(x - y) = G^{11}(x - y)$
- (ii) if x, y on C_2 $G(x - y) = G^{22}(x - y)$
- (iii) if x on C_1, y on C_2 $G(x - y) = G^{12}(x - y) = G^-(x^0 - y^0 + i\sigma, \vec{x} - \vec{y})$
- (iv) if x on C_2, y on C_1 $G(x - y) = G^{21}(x - y) = G^+(x^0 - i\sigma - y^0, \vec{y} - \vec{x})$

The cases when one (or both) of the time coordinates is on a vertical part of the contour are not explicitly needed when working in momentum space although the vertical pieces of the contour play a crucial role in deriving a consistent formalism [5, 6]. From the general expressions above one obtains the Fourier transforms:

$$\begin{aligned}
 D^{11}(K) &= \frac{i}{K^2 - m^2 + i\varepsilon} + 2\pi n_B(|k^0|) \delta(K^2 - m^2) \\
 D^{22}(K) &= -\frac{i}{K^2 - m^2 - i\varepsilon} + 2\pi n_B(|k^0|) \delta(K^2 - m^2) = (D^{11}(k))^* \\
 D^{12}(K) &= 2\pi(\theta(-k^0) + n_B(|k^0|)) \delta(K^2 - m^2) e^{\sigma k^0} \\
 D^{21}(K) &= 2\pi(\theta(k^0) + n_B(|k^0|)) \delta(K^2 - m^2) e^{-\sigma k^0}.
 \end{aligned} \tag{26}$$

Similar formulae can be derived for a fermion and they involve the Fermi-Dirac function $n_F(|k^0|) = 1/(e^{\beta|k^0|} + 1)$ rather than $n_B(|k^0|)$. A nice feature of the RTF is that it separates the temperature dependence contained in the statistical factors from the $T = 0$ part. In the RTF there is effectively a ‘‘doubling’’ of fields since one may introduce

$$\begin{aligned}
 \phi^1(x) &\equiv \phi(x) \text{ when } x \text{ is on the horizontal contour } C_1 \\
 \phi^2(x) &\equiv \phi(x - i\sigma) \text{ when } x \text{ is on the horizontal contour } C_2.
 \end{aligned} \tag{27}$$

This leads to two types of vertices: fields of type ϕ^1 couple together with strength $-ig$ or fields of type ϕ^2 couple with strength ig , the change of sign in the latter case arising because the time variable is running from right to left. The propagator in the RTF is a 2×2 matrix $\mathcal{D}(k) = (D^{ij}(k))$ with elements defined in eqs. (26). When calculating Green’s functions in this formalism it is necessary to sum over ‘‘type 1’’ and ‘‘type 2’’ internal vertices. This is crucial to cancel mathematically undefined terms, such as products of δ -functions with the same argument, which appear in intermediate stages of the calculation: to illustrate this point it is sufficient to consider self-energy insertions on a propagator and check that, only after summation over all types of internal vertices, terms of the form $(\delta(K^2 - m^2))^n$ disappear.

‘‘Cutting rules’’ for calculating the imaginary part of Green’s functions have been derived which are extremely useful to obtain rates or cross sections [7, 8]. The relation between RTF Green’s functions and the analytic continuation of ITF ones is neither trivial nor simple [9, 10, 11, 12] and has led to some confusion in the past [13, 14]. A nice way to relate the two, in some cases, is described next.

2.3 The R/A formalism

This formalism is a real-time formalism but it allows to construct directly retarded/advanced Green's functions, *i.e.* functions with external energies $(k_0 + i\varepsilon)$ or $(k_0 - i\varepsilon)$ which are related to the ITF Green's functions analytically continued as in eq. (25) [15, 16]. The basic step is the following decomposition of the RTF propagator

$$\mathcal{D}(K) = U(K) \begin{pmatrix} \Delta_R(K) & 0 \\ 0 & \Delta_A(K) \end{pmatrix} V(K) \quad (28)$$

where the retarded and advanced propagators are given by

$$\Delta_{R,A}(K) \equiv \frac{i}{K^2 - m^2 \pm i\varepsilon k^0}, \quad \varepsilon \rightarrow 0. \quad (29)$$

The matrices U and V depend on momentum K as well as the thermal factor and the parameter σ . They are associated to the RTF vertices and after summation on the two types of vertices one is led to the following momentum dependent vertices

$$\begin{aligned} g_{AAA}(P, Q, R) &= g_{RRR}(P, Q, R) = 0, \\ g_{RRA}(P, Q, R) &= g_{ARR}(P, Q, R) = g_{RAR}(P, Q, R) = g, \\ g_{RAA}(P, Q, R) &= -g (1 + n_B(q^0) + n_B(r^0)), \\ g_{ARA}(P, Q, R) &= -g (1 + n_B(p^0) + n_B(r^0)), \dots \end{aligned} \quad (30)$$

where the indices refer to the retarded/advanced prescriptions for the incoming external momenta P , Q and R . The first two equalities above express the KMS conditions in the R/A formalism. In loop calculations the sum over R and A internal indices is implied. Some useful discontinuity formulae to calculate cross sections have been derived in this formalism [15, 17].

3 Lepton pair production in a QCD plasma in perturbation theory

It is instructive to consider first the production of a lepton pair in a QCD plasma: this illustrates some of the features and problems occurring in thermal calculations [18, 19, 20]. When calculating this rate, at the first order in QCD, in hadronic collisions (*i.e.* at $T = 0$) it is well known that, at the partonic level, the infrared divergences (soft gluon) cancel according to the Lee-Kinoshita-Nauenberg theorem while the collinear divergences survive due to the collinear emission of a gluon by the annihilating quarks (process $q\bar{q} \rightarrow g\gamma^*$) or the collinear splitting of an initial gluon in the process $gq \rightarrow q\gamma^*$. However, the partons are confined and these divergences are absorbed, via the factorization theorem, in a re-definition of the structure functions of the hadrons which become scale dependent: in other words confinement shields these singularities. Since, in a quark-gluon plasma, the partons are deconfined, it is legitimate to ask what happens to the collinear singularities.

For a pair of invariant mass squared Q^2 , produced at rest, the rate is [21]:

$$\frac{dN}{dq_0 d^3 q d^4 x} = -\frac{\alpha}{12\pi^3} \frac{1}{Q^2} n_B(q_0) \text{Im } \Pi^\mu{}_\mu(Q). \quad (31)$$

where $\text{Im } \Pi^\mu{}_\mu(Q)$ is the imaginary part of the trace of the retarded photon self energy. It has been calculated at the first order in QCD in the RTF and the result was found to be finite, of the form [22, 23]:

$$\text{Im } \Pi^\mu{}_\mu(Q) = \frac{\alpha}{\pi} N_C \left(1 - 2n_F\left(\frac{Q}{2}\right)\right) Q^2 \left[1 + \frac{\alpha_s}{\pi} c_F \left(\frac{3}{4} + F\left(\frac{Q}{T}\right)\right)\right]. \quad (32)$$

In the above equation we have considered only one species of massless quarks of charge e ; α_s is the fine structure constant of the strong interactions and N_C and c_F are the usual colour factors. Except for an overall normalisation factor, the thermal dependence is contained in the function F . The calculation shows that both infrared and collinear divergences cancel in the $T = 0$ as well as in the thermal piece [18, 19, 20]. This occurs for two reasons: the phase space available at finite temperature is larger than at 0 temperature (one has to integrate over initial particle momenta) and processes such as $q\bar{q}g \rightarrow \gamma^*$ are included together with the usual annihilation and Compton diagrams of the Drell-Yan process (in this respect the factor 3/4 in the correction term of eq. (32) is exactly the factor appearing in the $T = 0$ annihilation of $e^+e^- \rightarrow q\bar{q}g$); secondly there exist relations among the Bose and Fermi statistical factors which express thermal equilibrium. For example, in equilibrium the rate of transition for a gluon of energy E_1 to be absorbed by a fermion of energy E_2 is the same as the rate for a fermion of energy $E_1 + E_2$ to decay into a gluon of energy E_1 and a fermion (detailed balance principle). This leads to relations of type

$$n_B(E_1)n_F(E_2) = n_F(E_1 + E_2)(1 + n_B(E_1) - n_F(E_2)) \quad (33)$$

and other similar relations. The cancellation of divergences has been explicitly shown to hold in scalar theories up to 3 loops [24] but no general proof exists (see however [25]). Recently it has been shown that the cancellation of singularities can also occur out of equilibrium [26]. The thermal correction factor has been calculated and it behaves as [22]

$$\begin{aligned} \frac{\alpha_s}{\pi} F\left(\frac{Q}{T}\right) &\equiv g^2 \frac{T^2}{Q^2}, & \text{as } \frac{T^2}{Q^2} \rightarrow 0 \\ \frac{\alpha_s}{\pi} F\left(\frac{Q}{T}\right) &\equiv g^2 \frac{T^2}{Q^2} \ln \frac{T^2}{Q^2}, & \text{as } \frac{T^2}{Q^2} \rightarrow \infty. \end{aligned} \quad (34)$$

This result can be understood as follows: the T^2 factor reflects the size of the thermal phase space while the $1/Q^2$ is necessary for dimensional reasons. When the lepton pair invariant mass becomes of order gT the perturbation series appears not to be well behaved as the correction term becomes as large as the lowest order one and when $Q^2 \rightarrow 0$ a divergence appears again. This illustrates a general feature of thermal field theories where perturbation theory breaks down when “soft” scales, *i.e.* scales of order gT , are involved. This is put in a rigorous way in the “Hard Thermal Loop” (HTL) resummation scheme of Braaten and Pisarski [27, 28] and Frenkel and Taylor [29, 30] to which we turn next. In this approach, it is natural to distinguish between “hard” scales, of $\mathcal{O}(T)$, the typical energies of quarks and gluons in the QCD plasma, from the soft scales, of $\mathcal{O}(gT)$, with the assumption $g \ll 1$.

4 Hard Thermal Loop Resummation

Consider, as an example, the retarded self-energy of a quark of momentum P in a QCD plasma. At the one-loop order, it can be expressed as

$$\begin{aligned}
 -i\Sigma_R(P) &= c_F g^2 \int \frac{d^4 L}{(2\pi)^3} \gamma_\nu (\not{P} + \not{L}) \gamma^\nu \left[\left(\frac{1}{2} + n_B(l_0) \right) \epsilon(l^0) \delta(L^2) \Delta_R(P+L) \right. \\
 &\quad \left. + \left(\frac{1}{2} - n_F(p_0 + l_0) \right) \epsilon(p^0 + l^0) \delta((P+L)^2) \Delta_A(L) \right]. \tag{35}
 \end{aligned}$$

If the external momentum P is soft, with components of $\mathcal{O}(gT)$, this expression reduces to

$$\Sigma_R(P) \sim \frac{c_F g^2}{4\pi^2} \int d\omega \omega (n_B(\omega) + n_F(\omega)) \int \frac{d\hat{L}}{2\pi} \frac{\hat{L}}{P\hat{L} + i\varepsilon} \tag{36}$$

where we have introduced the light-like vector $\hat{L} = (1, \hat{l})$ and $\omega = |l_0|$. The dimensional and the angular part of the loop integration factorize and it comes out [27]:

$$\Sigma_R(P) \sim \frac{m_q^2}{2} \int \frac{d\hat{L}}{2\pi} \frac{\hat{L}}{P\hat{L} + i\varepsilon}. \tag{37}$$

The factor m_q^2 results from the ω integration and it is

$$m_q^2 = c_F \frac{g^2 T^2}{8}. \tag{38}$$

The T^2 behavior arises entirely from the region where $\omega \sim T$, *i.e.* when the loop momentum is “hard”, the “soft” contribution of the loop being suppressed by factors of g . When inserting the self-energy correction on the fermion propagator the effective propagator is obtained:

$${}^*S_R(P) = \frac{i}{\not{P} - \Sigma_R(P)} \tag{39}$$

It is clear from eq. (37) that when P is soft the self-energy correction is also $\mathcal{O}(gT)$ and the modification implied by the loop is of the same order as the bare propagator. On the contrary when $P \sim T$ the self energy insertion induces a correction of $\mathcal{O}(g)$. As a consequence, for a consistent perturbative calculation, one should use the effective propagator eq. (39) when the momentum is soft while the bare one is sufficient when the momentum is hard. The pole in the propagator eq. (39) leads to complicated dispersion relations with two branches (quasi-particle excitations) and the fermion acquires an effective mass m_q at rest given by eq. (38); for hard momentum, one of the dispersion relations [31, 32] leads to a particle-like excitation of mass $2m_q$ whereas the other branch (called plasmino) decouples exponentially. An important consequence of thermal corrections is that the self energy acquires an imaginary part in the space-like region as can be seen by evaluating explicitly

$$\text{Im}\Sigma_R(P) = -\frac{m_q^2}{4} \int d\hat{L} \hat{L} \delta(P\hat{L}) \tag{40}$$

If $P^2 < 0$ then one immediately finds $\text{Im}\Sigma \sim gT$ while if $P^2 > 0$ it is vanishing, as the δ -function has no support (an exact calculation would give g^2T), and the quasi-particle interpretation is justified. The origin of the imaginary part when $P^2 < 0$ is the Landau damping effect which accounts for the scattering of quarks and gluons in the thermal bath. Such a mechanism has no equivalent at zero temperature where the imaginary part exists only above the threshold $P^2 > 0$.

In the same way one finds that the gluon propagator has a hard thermal loop contribution. In fact, in the Landau gauge, the effective gluon propagator takes the form [31, 33] (for simplicity, we do not specify the R/A indices)

$$*D^{\mu\nu}(L) \equiv -P_T^{\mu\nu}(L)\Delta^T(L) - P_L^{\mu\nu}(L)\Delta^L(L) \quad (41)$$

where

$$\Delta^{T,L}(L) \equiv \frac{i}{L^2 - \Pi_{T,L}(L)} \quad (42)$$

The tensors $P_{T,L}^{\mu\nu}(L)$ are the transverse and longitudinal projectors whose explicit expressions are found in [33]. The vanishing of the denominators implies different dispersion relations for the transverse and longitudinal polarisation states. One has the following limits:

$$\Pi_T(\omega, \vec{l} = 0) = \Pi_L(\omega, \vec{l} = 0) = m_g^2 = g^2T^2[N + N_f/2]/9 \quad (43)$$

which means that the gluon acquires an effective mass in the plasma. On the other hand, in the static limit,

$$\Pi_T(\omega = 0, \vec{l} \rightarrow 0) = 0 \quad (44)$$

$$\Pi_L(\omega = 0, \vec{l} \rightarrow 0) = 3m_g^2 \quad (45)$$

implying static screening of the electric field but not of the magnetic field.

Other Green's functions may receive hard loop corrections. For example, for the quark-quark-photon vertex (which we will need later) the HTL contribution is simply written as [27]

$$-ieV_\lambda(P, Q, R) = -ie\frac{m_q^2}{2} \int \frac{d\hat{L}}{2\pi} \frac{\hat{L}_\lambda \hat{L}}{P\hat{L} R\hat{L}} \quad (46)$$

where Q is the photon momentum and $\hat{L} = (1, \hat{l})$ is as in eq. (36). When the external momenta P, Q and R are soft the integrand is $\sim 1/(gT)^2$ and the one loop vertex is of $\mathcal{O}(e)$ as the bare QED vertex. On the contrary, if at least one of the external lines is hard the effective vertex is suppressed by at least one power of g . One is naturally led to introduce an effective vertex

$$\tilde{\Gamma}_\lambda(P, Q, R) = -ie(\gamma_\lambda + V_\lambda(P, Q, R)) \quad (47)$$

to be used, instead of the bare vertex, whenever all P, Q and R are soft.

Likewise it can be shown that the three-gluon vertex, and more generally the n -gluon vertex receive hard thermal loop corrections, as do Green's functions with 2-fermions and

$n - 2$ gauge bosons. Furthermore, in the HTL approximation the hard thermal loops are gauge invariant and they satisfy QED-like Ward identities [27]. For example, for the 3-gluon and the $q - \bar{q} - g$ vertex, respectively,

$$\begin{aligned} R^\lambda * \Gamma_{\lambda\mu\nu}(P, Q, R) &= - * D_{\mu\nu}^{-1}(P) + * D_{\mu\nu}^{-1}(R) \\ Q^\lambda * \tilde{\Gamma}_\lambda(P, Q, R) &= -i(* S^{-1}(P) + * S^{-1}(R)) \end{aligned} \quad (48)$$

In conclusion, when carrying out a perturbative calculation, to obtain a consistent result bare soft lines and vertices should be replaced by their effective counterparts: resummed propagators defined in eqs. (39,41) and effective vertices (*e.g.* eq. (47)). In Feynman diagrams effective Green's functions will be indicated by a \bullet to distinguish them from their bare counterparts. Two-loop corrections are not needed in this scheme since internal lines in self-energy and, more generally n -point functions, being hard, corrections to these will be suppressed by factors of g . These rules can be deduced systematically from an effective gauge-invariant lagrangian [34, 35]. The application of this scheme has lead to tremendous progress in the calculation of observables and to the solution of long standing puzzles.

5 Applications of the HTL resummation

We start by considering again the production of a soft virtual photon at rest [36]. As discussed before one should calculate the imaginary part of the vacuum polarisation diagram which, at lowest order, describes the annihilation of a soft quark-antiquark pair in a plasma. Since all momenta in the problem are soft one should use effective propagators and vertices and the graph to be considered is shown on Fig. 2. There exist other loop diagrams but, in principle, they do not contribute when summing over the photon polarisation indices. In terms of scattering amplitudes the graph of Fig. 2 has a very rich structure. Taking the imaginary part implies cutting through the effective vertices and propagators. Correspondingly, the rate of virtual photon production involves convolution of the diagrams in Fig. 3 [36]: if both internal fermion lines are time-like ($P^2, R^2 > 0$) the photon is produced in the annihilation or the decay of 2 quasi-particles (pole-pole) interaction (a); if one of the fermion line is space-like the imaginary part of the propagator corresponds to Landau damping and give rise to the scattering process (pole-cut) in (b); if both fermion lines are space-like then we obtain the double-scattering process (cut-cut) of (c). Cutting through effective vertices lead to similar diagrams (interference of (c) and (d)). The effect of Landau damping is of uttermost importance and increases the rate of production by several orders of magnitude compared to the estimates of eq. (32) [36].

Similarly the rate of production of a hard photon has been calculated and found to be finite in the HTL approach while it would be infinite at lowest order of perturbation theory [37, 38]: indeed, in the annihilation and Compton processes of Fig. 4a, the fermion propagator may diverge: for a static exchange, for example, one has to evaluate an integral of the form $\int dp/p$ which diverges for soft 3-momentum transfer p . In the HTL approach, the effective fermion propagator eq. (37) should be used leading to the integral $\int dp 8p/(8p^2 + m_q^2(4 + \pi^2))$ regularized

by the fermion thermal mass. The rate is then

$$q_0 \frac{dR^\gamma}{dq^3} \sim \frac{\alpha\alpha_s}{2\pi^2} T^2 e^{-q_0/T} \ln\left(\frac{q_0 T}{m_q^2}\right). \quad (49)$$

The calculation is much simpler than in the soft photon case as no effective vertices is needed since the vertices are connected to two hard lines: in fact it is sufficient to calculate the diagram of Fig. 4b where one of the internal lines at least is hard since the photon momentum is hard. Many more applications of the resummation scheme to the calculation of physical observables have been done [39].

There has been in the past much controversy concerning the gluon damping rate (*i.e.* the imaginary part of the gluon self-energy): a negative rate would mean undamped oscillations and a perturbatively unstable quark-gluon plasma. Until the HTL scheme was developed a wide range of gauge dependent results could be found in the literature, based on the one-loop approximation, with rates of different signs and strength [40]! These results were in fact incomplete since they used only bare soft propagators and vertices. Defining the damping rate of a transverse gluon at rest as $\gamma_T(0) = \text{Im}\Pi_T(m_g, 0)/2m_g$, and performing a consistent calculation in the effective theory involves the evaluation of the graphs of Fig. 5 with effective propagators and vertices [41]. The result comes out gauge invariant and positive:

$$\gamma_T(0) = \gamma_L(0) = 6.635 \frac{g^2 N_c}{24\pi} T \quad (50)$$

Among other successes one should mention the $\mathcal{O}(g^3)$ contribution to eq. (43) [42].

6 Problems in the HTL resummation

The use of the effective theory of Braaten and Pisarski makes it possible to improve the infrared behaviour of the theory in a gauge invariant manner. However there remains a number of difficulties related to the lack of static screening of transverse gluon modes (eq. (44)) and/or the appearance of collinear singularities when external particles are on-shell or massless. Two examples will respectively illustrate this problem: the damping rate of a fast moving particle and the production of soft real photons.

Consider a fast moving fermion with energy $p_0 \gg T$. Its damping rate is given in the effective approach by the imaginary part of the diagram of Fig. 6 with the dominant contribution arising from a soft transverse gluon and a hard internal fermion. The result is a convolution of the transverse gluon spectral function ρ_T (*i.e.* the imaginary part of $\Delta^T(L)$ in eq. (42) when $L^2 < 0$) and one finds

$$\gamma(P) \sim g^2 c_F T \int_{\text{soft}} l dl \int_{-l}^l \frac{dl_0}{l_0} \rho_T(l_0, l) \sim g^2 c_F T \int_{\text{soft}} \frac{dl}{l}. \quad (51)$$

This infrared divergence arises from unshielded static gluon exchanges (see eq. (44)). It should be noted that this divergence appears because one evaluates the diagram for an on-shell fermion, otherwise the off-shellness of the external fermion would shield the infrared

singularity. In QCD this IR divergence can be cured by the introduction of a magnetic mass (of non-perturbative origin) of $\mathcal{O}(g^2 T)$ [43, 44], a solution not applicable to QED where gauge invariance requires the magnetic mass to vanish. Several proposals have been considered to solve the problem. An interesting recent solution is based on the observation that higher loop diagrams with static transverse gluons contribute to the same order as the graph of Fig. 6. Such corrections have been resummed [45], in QED, by calculating the fermion propagator in a static background field and, defining the damping rate as the inverse of the decay time of the propagator in space-time coordinates, one finds

$$\gamma \sim g^2 T \ln\left(\frac{1}{g}\right). \quad (52)$$

Going back to momentum space the retarded fermion propagator $^*S_R(p_0, \vec{p})$ appears to be an entire function with singularity at $\text{Im}p_0 \rightarrow -\infty$.

The origin of the mass singularity problem can already be illustrated on a very simple example [46]. Coming back to eq. (37) and constructing $\text{Tr}(\gamma^0 \Sigma_R(P))$ it comes out

$$\text{Re Tr}(\gamma^0 \Sigma_R(P)) \sim -\frac{2}{p} m_q^2 \ln\left(\frac{p_0 - p}{p_0 + p}\right) \quad (53)$$

which diverges logarithmically for the massless on-shell condition. Such a singular behaviour occurs also in the photon or gluon polarisation tensor and higher order diagrams contribute to same order as the lowest order one [46]. Divergences like those in eq. (53) appear when calculating the production rate of soft real photons [47, 17]. The diagram to be calculated is that of Fig. 2 and taking the imaginary part implies “cutting” through an effective vertex (see an example in Fig. 7) *i.e.* taking the imaginary part of eq. (46) and therefore to evaluate an integral of type:

$$\text{Im}V_\lambda(P, Q, -R) \sim \frac{m_q^2}{2} \int \frac{d\hat{L}}{2\pi} \hat{L}_\lambda \hat{L} \frac{\delta(P\hat{L})}{R\hat{L}} \sim \frac{m_q^2}{2} \int \frac{d\hat{L}}{2\pi} \hat{L}_\lambda \hat{L} \frac{\delta(P\hat{L})}{Q\hat{L}} \quad (54)$$

where the constraint $P = R - Q$ has been used in the last equation. For a real photon, Q is light-like as is \hat{L} and therefore the above integral exhibits a collinear singularity when P and R are collinear since $P\hat{L}$ and $Q\hat{L}$ then vanish at the same point. Therefore, when applying strictly the HTL approach and keeping bare propagators and vertices when hard momenta are involved the production rate of soft real photon in a QCD plasma appears not to be defined. Even more interesting is the bremsstrahlung contribution to this rate [48, 49] which is supposed to vanish in the HTL approximation as it is contained in the gluon tadpole diagram: this diagram summarizes in fact the graphs of Fig. 8, where the internal momenta P and R are now hard and L is soft, and involves the evaluation of:

$$\text{Im} \Pi^\mu{}_\mu(Q) \sim e^2 g^2 q_0 \int d^4 P d^4 L \left(\frac{p}{l}\right)^2 n'_F(p_0) n_B(l_0) \rho_{T,L}(l_0, l) L^4 \frac{\delta(P^2) \delta((R+L)^2)}{R^2(P+L)^2}. \quad (55)$$

Using the δ -function constraints the term $1/R^2(P+L)^2$ naively appears of $\mathcal{O}(1/g^2 T^4)$ for P, R hard and L soft. However the denominator $R^2(P+L)^2$ is responsible for collinear divergences

which drastically modify this naive estimate. Using the constraints one easily rewrites

$$\frac{-4}{R^2(P+L)^2} = \frac{1}{P \cdot Q} \frac{1}{P \cdot Q + Q \cdot L} = \frac{1}{Q \cdot L} \left(\frac{1}{P \cdot Q} - \frac{1}{P \cdot Q + Q \cdot L} \right) \approx \frac{2}{Q \cdot L} \frac{1}{P \cdot Q}. \quad (56)$$

The first equality shows the presence of two very close collinear singularities (when $P \cdot Q=0$) since the two poles differ only by the soft $Q \cdot L$ term. The last equality holds true to leading order only after the integration over the whole phase space is performed. Introducing the angular variable $u = 1 - \cos \theta$ between the light-like momenta P and Q the above expression becomes, near $u = 0$,

$$\frac{1}{R^2(P+L)^2} \sim \frac{p}{qL^2} \frac{1}{pqu} \quad (57)$$

This form shows the presence of a logarithmic collinear divergence and the order of the residue at the pole in u is $1/g^4 T^4$ instead of the naively expected $1/g^2 T^4$. The near overlap of the collinear singularities causes the enhancement of the predicted rate by a factor $1/g^2$. The cross section is regularised by keeping the soft kinematic terms in the hard propagator of the diagrams as well as the hard fermion thermal mass [46] which enters the calculation at the same order. This discussion can be generalised to the case of the production of quasi-real photons at soft momenta and the relevant parameter is found to be Q^2/q_o^2 [49, 50]: when it is small ($< g^2$) the rate of production is enhanced by a factor $1/g^2$ compared to the expected order of magnitude in the HTL resummation program while when $Q^2/q_o^2 \sim 1$ the bremsstrahlung contribution is of the same order as that estimated in [36].

The implications of light-cone singularities for the HTL resummation program present an interesting challenge and they are still to be investigated [51].

7 Acknowledgements

I thank F. Gelis for many discussions and for much help in the preparation of these notes. I also thank the organisers of WHEPP 4 for a very enjoyable meeting.

References

- [1] A. Fetter, J. Walecka, Quantum Theory of Many Particle Systems, McGraw-Hill, New-York, 1971.
- [2] J.I. Kapusta, Finite-Temperature Field Theory, Cambridge University Press, 1989.
- [3] R. Mills, Propagators for Many-Particle Systems, Gordon and Breach Science Publishers, New-York, 1969.
- [4] N.P. Landsman, Ch.G. van Weert, Phys. Rep. **145**, 141 (1987).
- [5] T.S. Evans, Phys. Rev. D **47**, 4196 (1993).
- [6] F. Gelis, Z. Phys. C **70**, 321 (1996).
- [7] R.L. Kobes, G.W. Semenov, Nucl. Phys. B **260**, 714 (1985).
- [8] R.L. Kobes, G.W. Semenov, Nucl. Phys. B **272**, 329 (1986).

- [9] R.L. Kobes, Phys. Rev. D **42**, 562 (1990).
- [10] R.L. Kobes, Phys. Rev. Lett. **67**, 1384 (1991).
- [11] T.S. Evans, Nucl. Phys. B **374**, 340 (1991).
- [12] F. Gu erin, Nucl. Phys. B **432**, 281 (1994).
- [13] R. Baier, B. Pire, D. Schiff, Z. Phys. C **51**, 581 (1991).
- [14] H. Nakkagawa, A. Niegawa, H. Yokota, Phys. Lett. B **244**, 63 (1990).
- [15] P. Aurenche, T. Becherrawy, Nucl. Phys. B **379**, 259 (1992).
- [16] M.A. van Eijck, Ch.G. van Weert, Phys. Lett. B **278**, 305 (1992).
- [17] P. Aurenche, T. Becherrawy, E. Petitgirard, ENSLAPP-A-452/93, hep-ph/9403320.
- [18] J. Cleymans, I. Dadi , Z. Phys. C **45**, 57 (1989).
- [19] R. Baier, B. Pire, D. Schiff, Phys. Rev. D **38**, 2814 (1988).
- [20] T. Altherr, P. Aurenche, T. Becherrawy, Nucl. Phys. B **315**, 436 (1989).
- [21] C. Gale, J.I. Kapusta, Nucl. Phys. B **357**, 65 (1991).
- [22] T. Altherr, P. Aurenche, Z. Phys. C **45**, 99 (1989).
- [23] Y. Gabellini, T. Grandou, D. Poizat, Ann. of Phys. **202**, 436 (1990).
- [24] T. Grandou, M. Le Bellac, D. Poizat, Nucl. Phys. B **358**, 408 (1991).
- [25] A. Niegawa, Phys. Rev. Lett. **71**, 3055 (1993).
- [26] M. Le Bellac, H. Mabilat, Universit  de Nice preprint INLN-96/17.
- [27] E. Braaten, R.D. Pisarski, Nucl. Phys. B **337**, 569 (1990).
- [28] E. Braaten, R.D. Pisarski, Nucl. Phys. B **339**, 310 (1990).
- [29] J. Frenkel, J.C. Taylor, Nucl. Phys. B **334**, 199 (1990).
- [30] J. Frenkel, J.C. Taylor, Nucl. Phys. B **374**, 156 (1992).
- [31] V.V. Klimov, Sov. Phys. JETP **55**, 199 (1982).
- [32] H.A. Weldon, Phys. Rev. D **26**, 2789 (1982).
- [33] H.A. Weldon, Phys. Rev. D **26**, 1394 (1982).
- [34] J.C. Taylor, S.M.H. Wong, Nuc. Phys. **B346**, 115 (1990).
- [35] E. Braaten, R.D. Pisarski, Phys. Rev. D **45**, R1827 (1992).
- [36] E. Braaten, R.D. Pisarski, T.C. Yuan, Phys. Rev. Lett. **64**, 2242 (1990).
- [37] J.I. Kapusta, P. Lichard, D. Seibert, Phys. Rev. D **44**, 2774 (1991).
- [38] R. Baier, H. Nakkagawa, A. Niegawa, K. Redlich, Z. Phys. C **53**, 433 (1992).
- [39] M. Le Bellac, Thermal Field Theory, Cambridge University Press, 1996.
- [40] R.D. Pisarski, Nucl. Phys. A **525**, 175 (1991).
- [41] E. Braaten, R.D. Pisarski, Phys. Rev. D **42**, 2156 (1990).
- [42] H. Schultz, Nuc. Phys. B. **413**, 253 (1994).
- [43] A. Rebhan, Phys. Rev. D **46**, 482 (1992).
- [44] R.D. Pisarski, Phys. Rev. D **47**, 5589 (1993).
- [45] J.P. Blaizot, E. Iancu, Phys. Rev. Lett. **76**, 3080 (1996).
- [46] F. Flechsig, A.K. Rebhan, Nucl. Phys. B **464**, 279 (1996).
- [47] R. Baier, S. Peign , D. Schiff, Z. Phys. C **62**, 337 (1994).
- [48] P. Aurenche, F. Gelis, R. Kobes, E. Petitgirard , hep-ph/9606287.
- [49] P. Aurenche, F. Gelis, R. Kobes, E. Petitgirard , hep-ph/9609256.
- [50] F. Gelis, preprint ENSLAPP-A-613-96, hep-ph/9608429.
- [51] A. Rebhan, preprint TUW 96-15, hep-ph/9608410.

Figure Captions

Fig. 1 The real-time contour.

Fig. 2 Diagram in the resummed theory contributing to the production of soft photon in a quark-gluon plasma. All momenta are soft.

Fig. 3 The various processes involved in the evaluation of the diagram of the previous figure.

Fig. 4 (a) Processes contributing to hard photon production in a quark gluon plasma;
 (b) The corresponding diagram in the Braaten-Pisarski effective theory.

Fig. 5 Diagrams contributing to the gluon damping rate.

Fig. 6 The dominant diagram contributing to the damping rate of a fast fermion; the gluon in the loop is transverse.

Fig. 7 One of the diagram leading to a divergent contribution in the production of a soft real photon.

Fig. 8 The dominant bremsstrahlung diagrams for the production of a soft real photon.

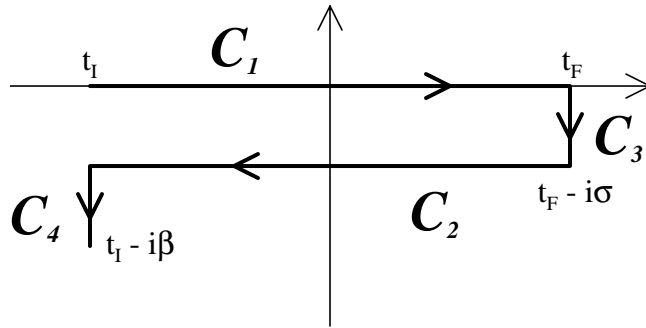


Fig. 1

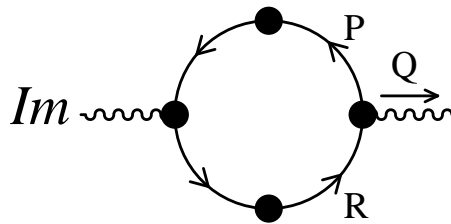


Fig. 2

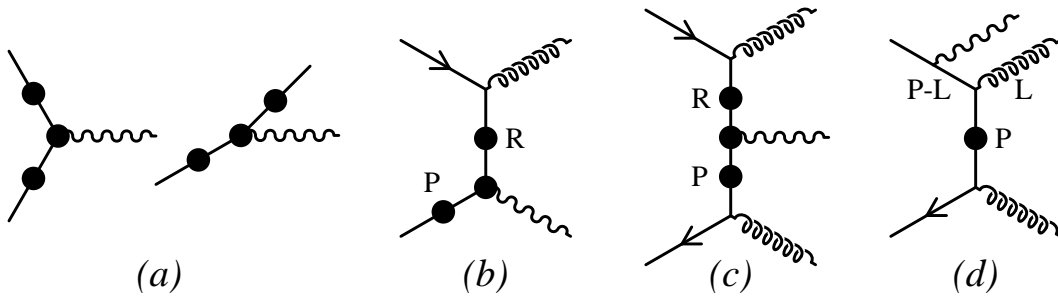


Fig. 3

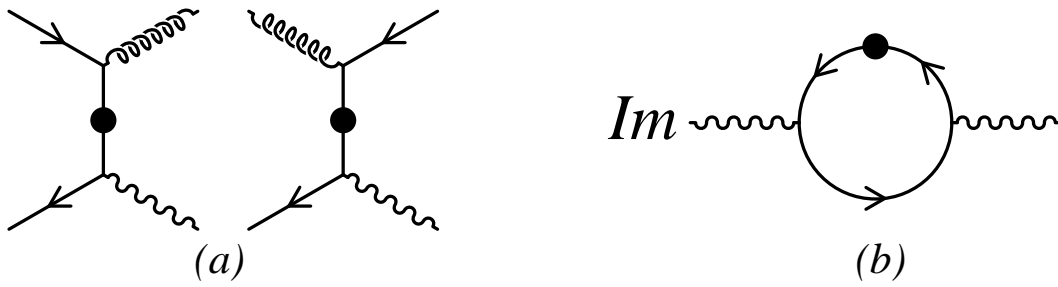


Fig. 4

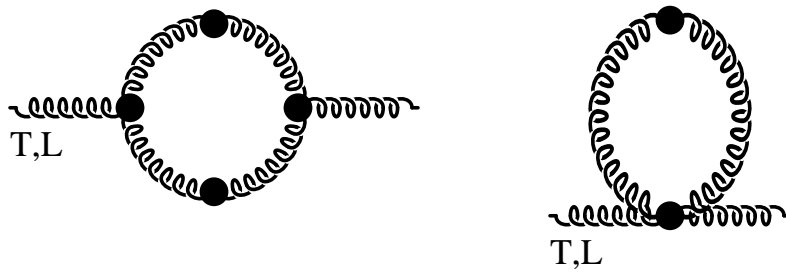


Fig. 5

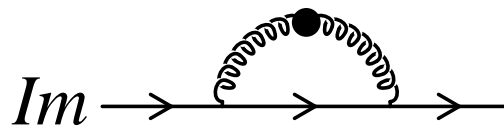


Fig. 6

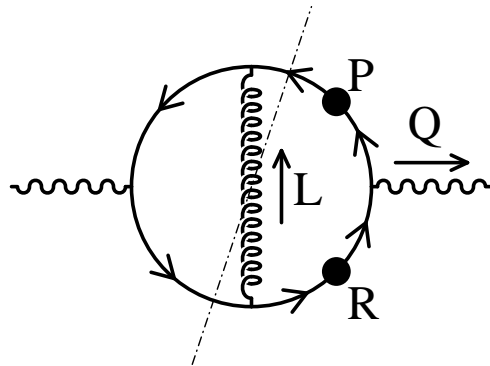


Fig. 7

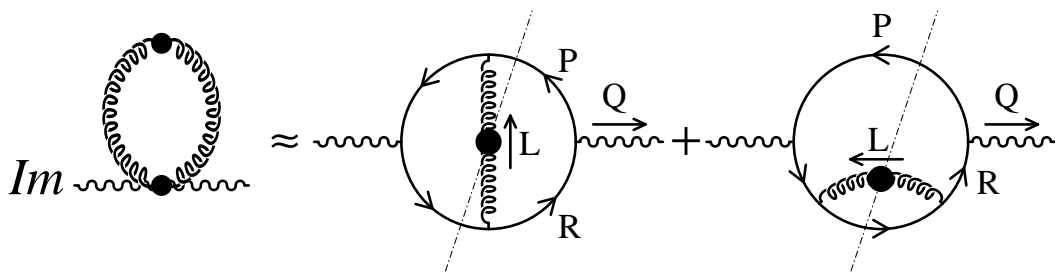


Fig. 8